Two-way coupling of the fully Lagrangian Approach with OpenFOAM for spray modelling

Oyuna Rybdylova*[,1], Timur Zaripov[1], Yuan Li[1]
[1]Advanced Engineering Centre, University of Brighton, BN2 4GJ, Brighton, UK
*Corresponding author: O.Rybdylova@brighton.ac.uk

Abstract
Accurate prediction of admixture distribution in space and in size is important for spray modelling in applications ranging from medical aerosols to fuel sprays in internal combustion engines. Modelling polydisperse sprays with inertial particles/droplets is particularly challenging as these types of flows may have trajectory crossing and caustics. The family of Eulerian-Eulerian methods are shown to be computationally expensive for these types of flow. The conventional approach to simulate admixture with low volume fraction is Lagrangian particle tracking, which implies direct calculation of the number of particles/droplets in a computational cell. The focus of this study is investigation of droplet dynamics and evaporation based on the Fully Lagrangian Approach (FLA). According to this method, particles/droplets are treated as a continuum (or a set of continua), which makes it possible to calculate particle/droplet number density from the continuity equation for the dispersed phase along chosen particle/droplet trajectory. The study is focussed on the implementation of two-way coupled FLA into open source CFD software OpenFOAM and generalisation of FLA for polydisperse flows. Both strands aiming to develop the FLA for wider use in engineering applications.
To take into account the effect of polydispersity of droplets, the continuity equation in the FLA has been generalised by introducing a new particle distribution function (PDF). This function represents the distribution of droplets over space, time and sizes. The set of Lagrangian variables in this case increases to include initial droplet size. This approach has been applied to a number of 1D and 2D flows of evaporating droplets with and without trajectory crossing.
The FLA has been implemented as part of OpenFOAM v6 Lagrangian library, allowing it to be used with all OpenFOAM solvers. A new steady-state two-way coupled 2D OpenFOAM solver has been developed and applied to test the FLA implementation in the case of gas-particle flow in a backward-facing step. The effect of mass loading of particles on the size of the recirculation zone has been shown.

Keywords
Droplets, Number density, Fully Lagrangian Approach, Polydispersity, OpenFOAM

Introduction

Gas-droplet flows are widely observed in engineering and environmental conditions [1], including during fuel injection in internal combustion engines [2]. In such flows, the admixture forms high concentration regions with folds (local zones of crossing particle/droplet trajectories, hereafter referred to as particles) and caustics. The Eulerian approaches cannot describe such regions with reasonable accuracy, since these approaches are based on the assumption of single-valued fields of the particle concentration and velocities. As shown by Healy and Young [3], the only method capable of calculating the particle concentration field in the case of multi-valued admixture parameter fields, without using excessive computer power, is the one suggested by Osiptsov [4], known as the Fully Lagrangian Approach (FLA). At the edge of a local region of crossing particle trajectories (caustics), the particle number density has a singularity. This is a well-known feature of the mathematical model of the collisionless continuum of point particles (see details in [5]). In the latter paper, typical examples of flows with singularities in the particle number density field were analysed. It was shown that for an integrable singularity of particle number density, at the singular points the mean distance between the particles remains finite and the model of collisionless particles remains valid. Our study is focused on further development of the Fully Lagrangian Approach (FLA) for the dispersed phase. The paper is arranged as follows: Section 1 is dedicated to the description of the generalised FLA (gFLA) and examples of application of gFLA; Section 2 covers implementation of the two-way coupled FLA in OpenFOAM.

The fully Lagrangian approach and its generalisation

In this section, only mathematical formalism for admixture in gas-droplet/particle flow is presented as this is the focus of the study. The carrier phase is described using a conventional approach such as an analytical or a numerical solution to Navier–Stokes equations.

FLA for monodisperse admixture

Following the Fully Lagrangian Approach [4], the Lagrangian variables are the initial coordinates of the droplet positions x_0, y_0, z_0. The continuity equation for the dispersed phase takes the form:

$$n_d \, |J| = n_{d0}, \tag{1}$$

where n_d is the droplet number density, $|J| \equiv |\det(J)|$ is the Jacobian of the transformation from Eulerian to Lagrangian coordinates $J_{ij} = \partial x_i / \partial x_{j0}$, indices i and j take the values of 1, 2, and 3, corresponding to x, y, and z coordinates. Since the volume fraction of admixture is small, the droplets are treated as a pressureless continuum [6]. The closed system of equations for the dispersed phase is presented as:

$$\begin{aligned} &n_d\,|J| = n_{d0}, \quad \frac{\partial \mathbf{x}_d}{\partial t} = \mathbf{v}_d, \quad \frac{\partial \mathbf{v}_d}{\partial t} = \mathbf{f}_d, \\ &c_{dl}\frac{\partial T_d}{\partial t} = q_d, \quad \frac{\partial J_{ij}}{\partial t} = q_{ij}, \quad \frac{\partial q_{ij}}{\partial t} = \frac{\partial f_{id}}{\partial x_{j0}}. \end{aligned} \tag{2}$$

Here $\mathbf{f}_d$ is the force exerted on a droplet, which is usually a known function of other parameters and the coordinates; q_d is the heat flux to the droplet, c_{dl} is the liquid heat capacity.

Dispersed phase radius vector $\mathbf{x}_d$, velocity $\mathbf{v}_d$, temperature T_d, and number density n_d are functions of x_0, y_0, z_0, and time t. For a chosen droplet trajectory, which corresponds to constant x_0, y_0, z_0, Equations (2) become a system of Ordinary Differential Equations with respect to time t. The initial conditions for Equations (2) correspond to the way the dispersed phase is introduced or fed to the flow.

Generalised FLA

The model described in the previous section can be generalised for the case of polydisperse particles [4]. The Lagrangian variables are the initial coordinates of the droplet positions x_0, y_0, z_0, and the initial size r_{d0}. The generalised continuity equation for the dispersed phase takes the form:

$$\tilde{n}_d\,(t, \mathbf{x}_d, r_d)\,|J| = \tilde{n}_{d0}, \tag{3}$$

Here, $\tilde{n}_d$ is a distribution of droplets over space, time and sizes, r_d is the droplet radius, $\mathbf{x} = (x, y, z)$ is a droplet position, $|J| \equiv |\det(J)|$ is the Jacobian of the transformation from Eulerian to Lagrangian coordinates with the following components:

$$J = \begin{pmatrix} J_{11} & J_{12} & J_{13} & J_{14} \\ J_{21} & J_{22} & J_{23} & J_{24} \\ J_{31} & J_{32} & J_{33} & J_{34} \\ J_{41} & J_{42} & J_{43} & J_{44} \end{pmatrix} = \begin{pmatrix} \partial x/\partial x_0 & \partial x/\partial y_0 & \partial x/\partial z_0 & \partial x/\partial r_{d0} \\ \partial y/\partial x_0 & \partial y/\partial y_0 & \partial y/\partial z_0 & \partial y/\partial r_{d0} \\ \partial z/\partial x_0 & \partial z/\partial y_0 & \partial z/\partial z_0 & \partial z/\partial r_{d0} \\ \partial r_d/\partial x_0 & \partial r_d/\partial y_0 & \partial r_d/\partial z_0 & \partial r_d/\partial r_{d0} \end{pmatrix} \tag{4}$$

For a chosen particle trajectory, we have the following system of ODE:

$$\begin{aligned} &\frac{\partial \mathbf{x}_d}{\partial t} = \mathbf{v}_d, \quad \frac{\partial \mathbf{v}_d}{\partial t} = \mathbf{f}_d, \\ &c_{dl}\frac{\partial T_d}{\partial t} = q_d, \quad \frac{\partial r_d}{\partial t} = \dot{r}_d, \\ &\frac{\partial J_{ij}}{\partial t} = q_{ij}, \quad \frac{\partial q_{ij}}{\partial t} = \frac{\partial f_{di}}{\partial x_k} J_{kj} + \frac{\partial f_{di}}{\partial r_d} J_{4j}, \quad i = 1,2,3, \quad j = 1, ..., 4 \\ &\frac{\partial J_{4j}}{\partial t} = \frac{\partial \dot{r}_d}{\partial x_{0j}} J_{4j}, \quad \frac{\partial J_{44}}{\partial t} = \frac{\partial \dot{r}_d}{\partial r_d} J_{44}, \quad i,j = 1,2,3. \end{aligned} \tag{5}$$

$\mathbf{f}_d$ is the force exerted on a droplet, which is usually a known function of the droplet size, droplet velocity, and other parameters; $\dot{r}_d$ is rate of droplet size change, which is usually a known function of the droplet size and thermodynamic parameters, q_d is the heat flux to the droplet, c_{dl} is the liquid heat capacity, the values of 1, 2, and 3 correspond to x, y, and z coordinates respectively.

The following two sections describe examples of application of the gFLA to 1D and 2D flows.

1D quiescent carrier phase

Consider an injection of droplets into a still hot air with uniform temperature T_a, droplets injected with the same velocity U and temperature T_0.

The force and heat flux on the droplet are presented as follows:

$$\begin{aligned} &\mathbf{f}_d = 6\pi r_d^* \mu\,(\mathbf{v}^* - \mathbf{v}_d^*)\,, \\ &q_d = 4\pi r_d^* \lambda (T^* - T_d^*). \end{aligned} \tag{6}$$

Assume all the heat that reaches droplet surface is spent on evaporation of the droplet, then

$$\dot{m} = \frac{q_d}{H},$$

where H is the latent heat of evaporation of the droplet liquid.

The following non-dimensional parameters are introduced:

$$\begin{aligned} &x_{(d)} = \frac{x_{(d)}^*}{l_\tau},\ u_{(d)} = \frac{u_{(d)}^*}{U},\ t = \frac{U t^*}{l_{\tau 0}},\ r_d = \frac{r_d^*}{r_0},\ \tilde{n}_d = \frac{\tilde{n}_d^*}{n_{dt0}}, \\ &T(T_s) = \frac{T^*(T_s^*) - T_0}{T_a - T_0}. \end{aligned} \tag{7}$$

where the carrier phase (parameters without subscript) and the dispersed phase (with subscript '$_d$') coordinates and velocities are normalised using the droplet velocity relaxation length $l_{\tau 0}$ corresponding to the characteristic droplet radius r_0 and droplet initial velocity U; n_{dt0} – total initial droplet number density at x_0, where the droplets are injected; the so-defined dimensionless temperature takes values between 0 and 1, with 0 corresponding to the droplet injection temperature.

$$l_{\tau 0} = \frac{m_0 U}{6\pi r_0 \mu},\ m_0 = \frac{4}{3}\pi r_0^3 \rho_{dl},$$

where ρ_{dl} is the droplet liquid density.
For 1D case, Equations (3)–(5) take form:

$$\tilde{n}_d\left(t, x, r_d\right)|J| = \tilde{n}_{d0}, \tag{8}$$

$$J = \begin{pmatrix} J_{11} & J_{12} \\ J_{21} & J_{22} \end{pmatrix} = \begin{pmatrix} \partial x/\partial x_0 & \partial x/\partial r_{d0} \\ \partial r_d/\partial x_0 & \partial r_d/\partial r_{d0} \end{pmatrix} \tag{9}$$

$$\begin{aligned}
&\frac{dx_d}{dt} = u_d, \quad \frac{du_d}{dt} = -\frac{1}{r_d^2}u_d, \\
&T_d = 0, \quad \frac{dr_d^2}{dt} = -\delta, \\
&\frac{dJ_{11}}{dt} = q_{11}, \quad \frac{dJ_{12}}{dt} = q_{12}, \\
&\frac{dq_{11}}{dt} = -\frac{1}{r_d^2}q_{11} + \frac{2}{r_d^3}u_d J_{21}, \quad \frac{dq_{12}}{dt} = -\frac{1}{r_d^2}q_{12} + \frac{2}{r_d^3}u_d J_{22} \\
&\frac{dJ_{21}}{dt} = 0, \quad \frac{dJ_{22}}{dt} = \frac{\delta}{2r_d^2}J_{22} \\
&\delta = \frac{4}{9}\frac{\lambda\left(T_a - T_0\right)}{\mu H}.
\end{aligned} \tag{10}$$

Assume that the initial distribution of droplet sizes at x_0 is log-normal:

$$\tilde{n}_{d0} = \frac{1}{r_d}\frac{1}{S\sqrt{2\pi}}\exp\left(-\frac{\left(\ln r_d - M\right)^2}{2S^2}\right),$$

where $M = 0.16$ and $S = 0.4$ are mean and variance for the corresponding normal distribution, see Fig. 1.

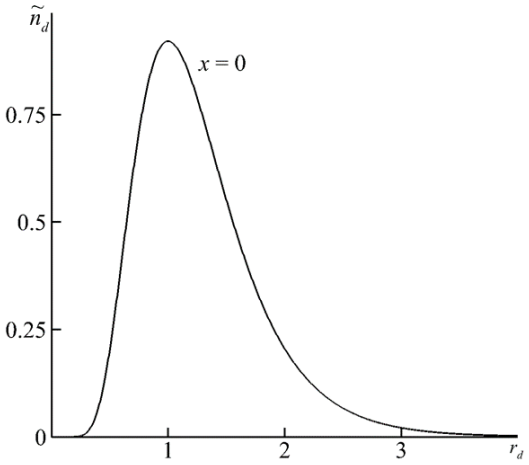

Figure 1. Normalised droplet size distribution.

In the case of stationary flow, the the system (8)– (10) can be reduced to

$$\tilde{n}_d\left(t, x, r_d\right)\begin{vmatrix} u_d & \partial x/\partial r_{d0} \\ \dot{r} & \partial r_d/\partial r_{d0} \end{vmatrix} = \tilde{n}_{d0} u_{d0}, \tag{11}$$

$$
\begin{aligned}
&\frac{dx_d}{dt} = u_d, \quad \frac{du_d}{dt} = -\frac{1}{r_d^2}u_d, \\
&T_d = 0, \quad \frac{dr_d^2}{dt} = -\delta, \\
&\frac{dJ_{12}}{dt} = q_{12}, \quad \frac{dq_{12}}{dt} = -\frac{1}{r_d^2}q_{12} + \frac{2}{r_d^3}u_d J_{22} \\
&\frac{dJ_{22}}{dt} = \frac{\delta}{2r_d^2}J_{22} \\
&\delta = \frac{4}{9}\frac{\lambda\,(T_a - T_0)}{\mu H}.
\end{aligned}
\tag{12}
$$

The initial conditions for System (10) are:

$$
\begin{aligned}
&x = x_0, u_d = 1, T_d = 0, \tilde{n}_d = \tilde{n}_{d0}, r_d = r_{d0} \\
&J_{12} = 0, \quad J_{22} = 1, \quad q_{12} = 0.
\end{aligned}
\tag{13}
$$

System (12) can be solved analytically. The analytical solution is used to test numerical calculations. The solution is

$$
\begin{aligned}
&x_d = \frac{r_{d0}^2}{\delta + 1}\left[1 - \left(1 - \frac{\delta t}{r_{d0}^2}\right)^{\frac{\delta+1}{\delta}}\right], \\
&u_d = \left(\frac{r_d}{r_{d0}}\right)^{2/\delta} = \left(1 - \frac{\delta t}{r_{d0}^2}\right)^{1/\delta}, \\
&r_d^2 = r_{d0}^2 - \delta t, \\
&J22 = \frac{r_{d0}}{r_d}, \\
&J12 = -\frac{2}{r_{d0}}\left(1 - \frac{\delta t}{r_{d0}^2}\right)^{1/\delta} t, \\
&\tilde{n}_d = \tilde{n}_{d0}\left(1 - \frac{\delta t}{r_{d0}^2}\right)^{-1/2} = \tilde{n}_{d0}\frac{r_{d0}}{r_d}
\end{aligned}
\tag{14}
$$

The results are presented in Fig. 2, for $\delta = 1$. As expected, smaller droplets relax to the stationary flow quicker that the larger droplets (Fig. 2 left). As droplets evaporate, the maximum of the distribution functions shifts to the left (Fig. 2 right) and its value decreases.

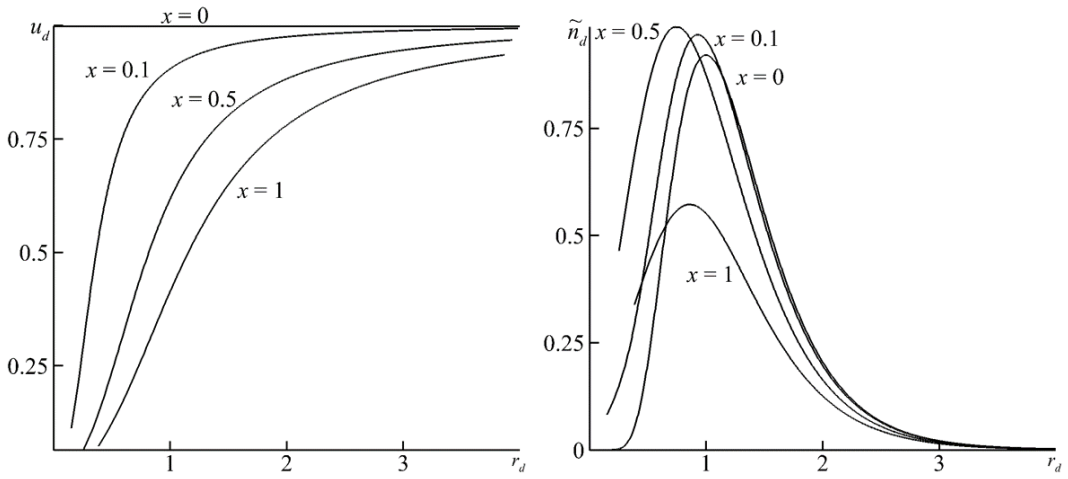

Figure 2. Profiles at various cross-sections: velocity distribution against size (left); distribution function against size (right)

2D spray injection in cross-flow

Consider an injection of droplets into a hot air with uniform temperature T_a and constant velocity U, droplets injection forms a 90 $^\circ$–jet with constant velocity magnitude U_j^* and temperature T_0.

The force and heat flux on the droplet are as before, see Equations (6). Same as earlier, we assume that all the heat that reaches droplet surface is spent on evaporation of the droplet.

If the characteristic length is taken equal to droplet velocity relaxation length, then the non-dimensional parameters are introduced as:

$$\begin{aligned} &x_{(d)} = \frac{x^*_{(d)}}{l_{\tau 0}},\ u_{(d)} = \frac{u^*_{(d)}}{U},\ t = \frac{Ut^*}{l_{\tau 0}},\ r_d = \frac{r^*_d}{r_0},\ \tilde{n}_d = \frac{\tilde{n}^*_d}{n_{dt0}}, \\ &T(T_s) = \frac{T^*(T^*_s) - T_0}{T_a - T_0},\ l_{\tau 0} = \frac{m_0 U_m}{6\pi r_0 \mu},\ m_0 = \frac{4}{3}\pi r_0^3 \rho_{dl}, \end{aligned} \tag{15}$$

n_{dt0} – total initial droplet number density at x_0, where the droplets are injected; the so-defined dimensionless temperature takes values between 0 and 1, with 0 corresponding to the droplet injection temperature, ρ_{dl} is the droplet liquid density, the droplet velocity relaxation length $l_{\tau 0}$ corresponds to the characteristic droplet radius r_0 and gas velocity U.
System (5) can be simplified for 2D steady-state flows and it takes form:

$$\tilde{n}_d\left(t, x, r_d\right)\left|\det\begin{pmatrix} J_{11} & u_d & J_{13} \\ J_{21} & v_d & J_{23} \\ J_{31} & \dot{r} & J_{33} \end{pmatrix}\right| = \tilde{n}_{d0} v_{d0}, \tag{16}$$

For horizontal flow of the carrier phase and $\beta = 1$, the system of ODEs takes form:

$$\begin{aligned} &\frac{dx_d}{dt} = u_d, \quad \frac{dy_d}{dt} = v_d, \quad \frac{du_d}{dt} = \frac{1}{r_d^2}\left(1 - u_d\right), \quad \frac{dv_d}{dt} = -\frac{1}{r_d^2} v_d, \\ &T_d = 0, \quad \frac{dr_d^2}{dt} = -\delta, \\ &\frac{dJ_{11}}{dt} = q_{11}, \quad \frac{dJ_{13}}{dt} = q_{13}, \\ &\frac{dJ_{21}}{dt} = q_{21}, \quad \frac{dJ_{23}}{dt} = q_{23}, \\ &\frac{dq_{11}}{dt} = -\frac{1}{r_d^2} q_{11} - \frac{2}{r_d^3}\left(1 - u_d\right) J_{31}, \\ &\frac{dq_{13}}{dt} = -\frac{1}{r_d^2} q_{13} - \frac{2}{r_d^3}\left(1 - u_d\right) J_{33}, \\ &\frac{dq_{21}}{dt} = -\frac{1}{r_d^2} q_{21} + \frac{2}{r_d^3} v_d J_{31}, \\ &\frac{dq_{23}}{dt} = -\frac{1}{r_d^2} q_{23} + \frac{2}{r_d^3} v_d J_{33}, \\ &\frac{dJ_{31}}{dt} = 0, \quad \frac{dJ_{33}}{dt} = \frac{\delta}{2 r_d^2} J_{33}, \\ &\delta = \frac{4}{9}\frac{\lambda\left(T_a - T_0\right)}{\mu H} \end{aligned} \tag{17}$$

Corresponding initial conditions are:

$$\begin{aligned} &x = x_0 \in [-\epsilon, \epsilon],\ y = 0,\ u_d = U_j \cos\left(-\frac{\pi}{4}\cdot\frac{x_0}{\epsilon} + \frac{\pi}{2}\right),\ v_d = U_j \sin\left(-\frac{\pi}{4}\cdot\frac{x_0}{\epsilon} + \frac{\pi}{2}\right), \\ &T_d = 0, \tilde{n}_d = \tilde{n}_{d0}, r_d = r_{d0} \\ &J_{11} = 1,\ J_{13} = 0,\ J_{21} = 0,\ J_{23} = 0,\ J_{31} = 0,\ J_{33} = 1, \\ &q_{11} = \frac{1}{\epsilon}\frac{\pi}{4} U_j \cos\left(\frac{\pi}{4}\frac{x_0}{\epsilon}\right),\ q_{13} = 0,\ q_{21} = -\frac{1}{\epsilon}\frac{\pi}{4} U_j \sin\left(\frac{\pi}{4}\frac{x_0}{\epsilon}\right),\ q_{23} = 0. \end{aligned} \tag{18}$$

The initial distribution of droplet sizes at is assumed to be the same as in the previous example.
The results are presented in Fig. 3, for $\delta = 1$ and $\beta = 1$. On the left Figure, the size of the marker is proportional to the size of the droplet, colour denotes distribution function of droplets. On the right Figure, one can see the total number density, which is obtained after integration over all sizes at each point. As expected, as droplets are carried by the cross flow and evaporate, the distribution of droplets shifts to the right and total number decreases.

Two-way coupled Fully Lagrangian approach

The carrier phase is modelled as an incompressible or compressible viscous flow of gas described by the mass continuity and Navier–Stokes equations. In the case of an incompressible flow these equations are presented as

$$\nabla \cdot \mathbf{u} = 0, \tag{19}$$

$$\rho\frac{\partial \mathbf{u}}{\partial t} + \rho(\mathbf{u}\cdot\nabla)\mathbf{u} = -\nabla p + \mu\nabla^2\mathbf{u} + S_u, \tag{20}$$

where ρ is the gas density, $\mathbf{u}$ is the gas velocity, p is the static pressure, μ is the gas dynamic viscosity, S_u is the source term due to momentum exchange with dispersed phase.

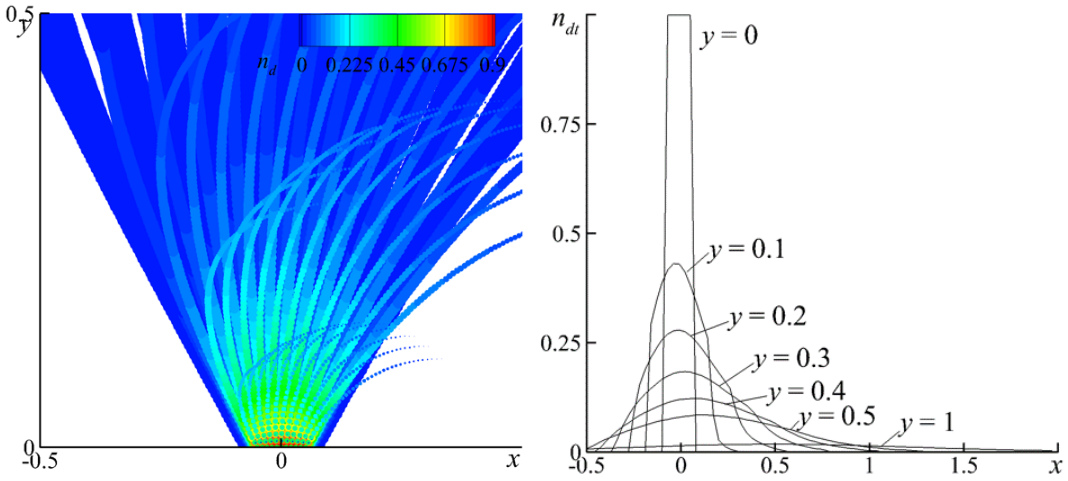

Figure 3. Droplet trajectories and distribution function (left); total number density at various cross-sections (right).

Flow Reynolds number is defined as

$$\mathrm{Re} = \frac{\rho L U}{\mu}, \tag{21}$$

where L and U are characteristic length and velocity scales.
The dispersed phase is modelled using FLA for monodisperse admixture [4]. Inertial behaviour of particles is determined by the Stokes number

$$\mathrm{Stk} = \frac{\tau_\mathrm{d}}{\tau_\mathrm{f}}, \tag{22}$$

where τ_f is the characteristic flow time, and particle response time τ_d is estimated as

$$\tau_\mathrm{d} = \frac{\rho_\mathrm{d} d_\mathrm{d}^2}{18\mu}. \tag{23}$$

Coupling of phases
The contribution of a single particle to Eq.20 is written as

$$S_{\mathrm{u,d}} = -\frac{\rho\alpha n_d}{m_d}\frac{d\mathbf{v}}{dt} = -\frac{\rho\alpha n_d}{m_d}\beta(\mathbf{u}-\mathbf{v}), \tag{24}$$

where m_d is the mass of a droplet.
In the steady-state case the collective source term for all the trajectories passing through control volume is calculated as

$$S_{\mathrm{u,cv}} = -\frac{\rho}{n_\mathrm{traj}}\sum_{j}^{n_\mathrm{traj}}\frac{\alpha_j\beta_j}{m_{d,j}}\sum_{i}^{n_{\mathrm{cv},j}} n_{d,\mathrm{ji}}(\mathbf{u}_{ji}-\mathbf{v}_{ji}), \tag{25}$$

where n_traj is the number of trajectories passing though the cell, $n_{\mathrm{cv,j}}$ is the number of points along the trajectory j in current control volume.
This model has been implemented into open-source CFD code OpenFOAM v6.

Back-facing step flow
As test case for the new solver, a laminar steady-state flow of air with inertial particles over back-facing step has been used. Scheme of computational domain is shown in Fig.4. Boundary conditions are set as follows: AB is velocity inlet, EF is pressure outlet, BC, CD, DE and AF are walls. As in [7], ratio $(\mathrm{EF})/\mathrm{AB} = 1.9423$ and $L = 2{*}\mathrm{AB}$ is a characteristic length in Eq. 21. To have a consistent Re and Stk dimensional velocity at inlet has been fixed at $\mathrm{U} = 0.03\mathrm{m\,s}^{-1}$. All results presented below are for the case with $\mathrm{Re} = 50$ and $\mathrm{Stk} = 0.5$. For this case, coupled and uncoupled solution were calculated. Results of the calculations for the uncoupled flow were verified against reference numerical solutions and experimental studies [7, 8].
Dimensional velocity magnitude of the air for the coupled solution and samples of values of number density n_p along trajectories are shown in Fig.5 at the top and bottom figures respectively. It can be seen, that number density has tendency to increase in the areas where flow slows down (centre of the stream), and decrease in the areas where flow speeds up (along the boundary layer and recirculation region behind the back-facing step).
Profiles of the dimensional air velocity in x-direction u_x^* along the vertical lines are shown in Fig.6. Solid line corresponds to the uncoupled solution, dashed line corresponds to the two-way coupled solution. The the u_x^* profile

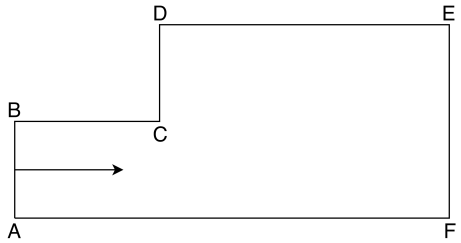

Figure 4. Calculation domain.

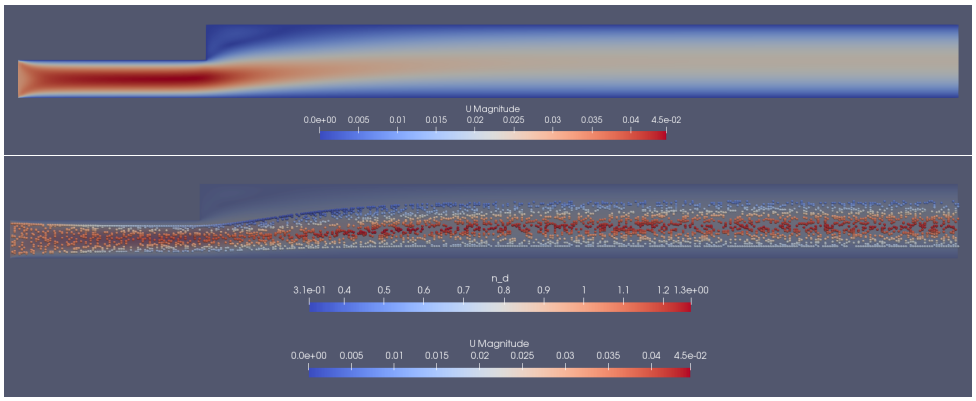

Figure 5. Velocity magnitude (top) and particle number density samples (bottom).

of the uncouples solution tends to symmetrical shape faster than the two-way coupled one. Inertia of the particles keeps this profile asymmetrical and maximal u_x^* in the stream higher for the two-way coupled solution.
Profiles of the dimensional air velocity in x-direction u_x^* along the horizontal line $y = 0.95 * \mathrm{EF}$ are shown in Fig.7. Solid line corresponds to the uncoupled solution, dashed line corresponds to the two-way coupled solution. Points, where the lines cross $y = 0$, correspond to the end of recirculation zone. In can be seen, that the recirculation zone is bigger for two-coupled case compared to uncoupled one, which is due to higher flow velocity in the stream.

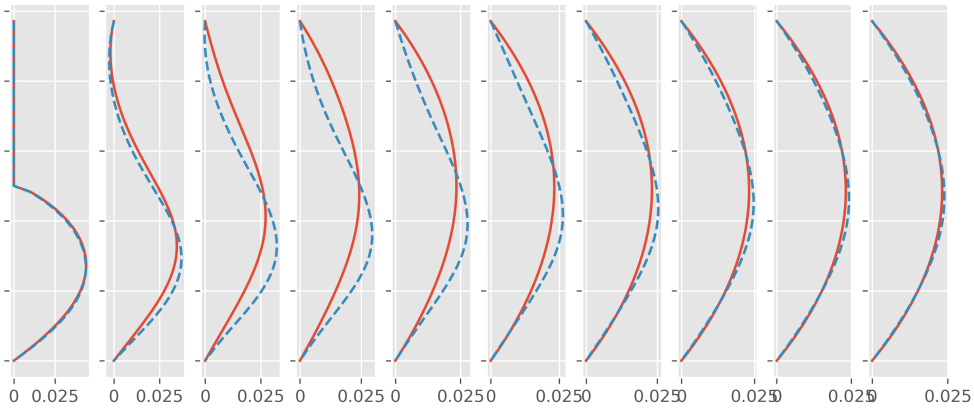

Figure 6. u_x^* profiles along the vertical lines.

Conclusion

Two-way momentum coupled model of gas-particle flow has been developed and implemented into OpenFOAM. Predictions of the new model have been compared to uncoupled flow for the case of back-facing step flow. Comparison have showed significant effect of the coupling on the horizontal velocity profiles and the size of recirculation zone.
The Fully Lagrangian approach has been developed to take into account polydispersity and evaporation/condensation of droplets, and has been tested in simple case studies. Further work is required to couple gFLA with OpenFOAM to enable simulations of more complex flows.

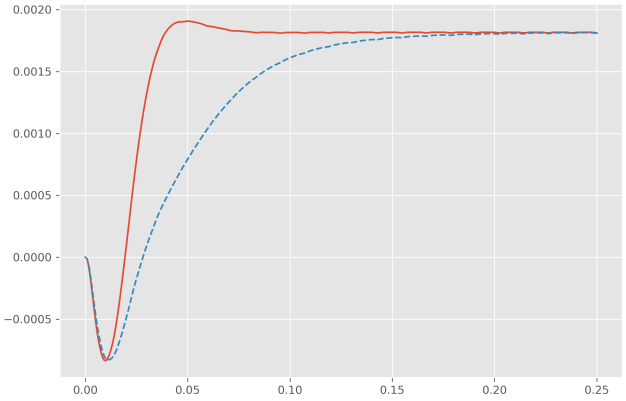

Figure 7. u_x^* profiles along the horizontal line $y = 0.95 * \mathrm{EF}$.

Acknowledgements
The authors are grateful to the EPSRC, UK (Grant no. EP/R012024/1) for their financial support.

Nomenclature

$\mathbf{f}_d$	aerodynamic drag force
FLA	Fully Lagrangian Approach also known as Osiptsov's method [4]
J	Jacobian and Jacobian components
m	mass of a particle/droplet of radius σ
n_d	particle/droplet number density
q	denote partial derivatives of Jacobian components with respect to Lagrangian coordinates 5
t	time $[\mathrm{s}]$
$\mathbf{v} = (u, v)$	velocity
U	axial velocity used in defining the SDV model
r	droplet radius
$\mathbf{x} = (x, y)$	position vector
α	mass fraction of admixture
β	droplet inertia parameter
δ	droplet evaporation parameter
μ	dynamic viscosity $[\mathrm{Pa\ s}]$
ρ	density $[\mathrm{kg\ m^{-3}}]$
Subscripts	
d	aerodynamic drag
d	dispersed phase parameter
i, j	indices
0	initial value
Superscripts	
$*$	dimensional parameter

References

[1] Sazhin, S. S., 2014, "Droplets and Sprays". Springer.
[2] Begg, S., Kaplanski, F. B., Sazhin, S. S., Hindle, M., and Heikal, M., 2009, *International Journal of Engine Research*, 10 (4), pp. 195-214.
[3] Healy, D. P., and Young, J. B., 2005, *Proceedings of the Royal Society of London A: Mathematical, Physical and Engineering Sciences*, 461 (2059), pp. 2197-2225.
[4] Osiptsov, A. N., 2000, *Astrophysics and Space Science*, 274 (1-2), pp. 377-386.
[5] Osiptsov, A. N., 1984, *Fluid Dynamics*, 19 (3), pp. 378-385.
[6] Marble F.E., 1970, *Annual Review of Fluid Mechanics*, 2, pp. 397-446.
[7] Biswas, G., Breuer, M. and Durst, F., 2004. *Journal of fluids engineering*, 126(3), pp.362-374.
[8] Armaly, B. F., Durst, F., Pereira, J. C. F. and Schönung, B., 1983. *Journal of fluid Mechanics*, 127, pp.473-496.